Direct Observation of Sub-Binomial Light

Tim J. Bartley,[1] Gaia Donati,[1] Xian-Min Jin,[1,2] Animesh Datta,[1] Marco Barbieri,[1] and Ian A. Walmsley[1]

[1]*Clarendon Laboratory, University of Oxford, Parks Road, Oxford OX1 3PU, United Kingdom*
[2]*Department of Physics, Shanghai Jiao Tong University, Shanghai 200240, People's Republic of China*

Nonclassical states of light are necessary resources for quantum technologies such as cryptography, computation and the definition of metrological standards. Observing signatures of nonclassicality generally requires inferring either the photon number distribution or a quasiprobability distribution indirectly from a set of measurements. Here, we report an experiment in which the nonclassical character of families of quantum states is assessed by direct inspection of the outcomes from a multiplexed photon counter. This scheme does not register the actual photon number distribution; the statistics of the detector clicks alone serve as a witness of nonclassicality, as proposed by Sperling *et al.* [Phys. Rev. Lett. **109**, 093601 (2012)]. Our work paves a way for the practical characterization of increasingly sophisticated states and detectors.

PACS numbers: 42.50.Ar, 42.50.Dv, 42.50.Xa

States of the electromagnetic field with no analogue in a classical theory of electromagnetism provide a means to characterize quantum coherence and are a valuable resource for quantum-enhanced technologies. Determining what constitutes a nonclassical state is not a trivial matter. Many criteria to establish where the quantum-classical boundary lies have been proposed. Typically, one considers pathological behaviors of distributions in phase space: one looks for negative values of the Wigner quasiprobability function on the quadrature space [1], or values more singular than a delta function of the Glauber-Sudarshan P distribution on the phase-amplitude space [2–4], with the latter definition covering a larger class of states. When detecting photons directly, the Mandel parameter Q_M is often used [5]. This neatly captures any sub-Poissonian behavior in the photon statistics as a witness of nonclassicality.

Experimentally, these criteria have been widely adopted, and inferred either by full reconstruction of the distribution [6–10], or by direct measurement [11,12]. A different approach consists of examining the photon number distribution in a counting experiment [5,13–18]. While actual photon number resolving detectors are becoming more frequently available [19–22], simpler solutions are still appealing as quantum networks become more complex. Multiplexed detectors are a commonplace choice for accessing higher order Fock states by binning the light to several on-off detectors [23,24]. As such, these detectors do not output the photon number distribution. It is recognized that the Mandel parameter applied to the click distribution would give false indications of nonclassicality even for a large number of detection bins [25]. A linear inversion technique is then required [11,26–28] in order to obtain the actual distribution from the distribution of the clicks. However, this becomes more sensitive to noise and less tractable with increasing system size.

In this Letter, we directly observe a signature of nonclassicality in the output of a time-multiplexed detector, following the proposal in Ref. [29] which identifies a subbinomial behavior in the click statistics. We experimentally measure this sub-binomial character for three families of quantum states and compare it with the standard Mandel parameter [5], as well as a naïve analysis of the data. Our results show that the sub-binomial behavior of click statistics is a reliable indicator of nonclassicality of single-mode light fields. Moreover, this test performs just as well at inferring the true Mandel parameter from the photon distribution. As quantum information systems evolve in sophistication, characterization via full tomography becomes prohibitively expensive, and our results pave the way for a simple characterization of quantum states and detectors.

The general scheme of a multiplexed detector is illustrated in Fig. 1(a). These simple devices permit access to more detail about the number distribution of a light field through sequential division of an input beam on a series of beam splitters, with detection of each output mode by avalanche photodiodes (APDs). Different architectures have been realized by using either spatial [Fig. 1(b)] [30] or time-bin [Fig. 1(c)] [31] multiplexing. In this way, APDs with no photon number resolving capabilities can still deliver information about an input state with $n > 1$ photons. However, this is nondeterministic, occurring only when the photons split into N separated spatial or temporal bins. This means that the distribution of the photons $\{p_n\}$, and the one of the clicks from the APDs $\{c_i\}$ are different, and their difference only scales with the number of bins as $1/N$ [25]. Some characterization of the device is required to find the matrix relating the two distributions. Since the splitting operates a linear transformation, the matrix can be inverted in order to obtain the values of $\{p_n\}$ [11,24,32]. In our realization, we adopt a time-multiplexed detector (TMD) which can detect up to $N = 8$ events by splitting
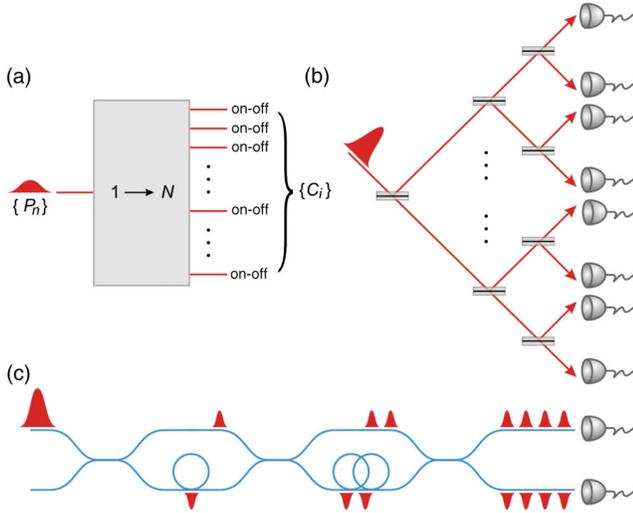
FIG. 1 (color online). (a) General scheme of a multiplexed detector. Access to more detail of the photon distribution is obtained by dividing the input beam onto several modes, which are then measured with on-off detectors, such as APDs. The photon number distribution $\{p_n\}$ determines the statistics of the counts $\{c_i\}$, i.e., the probabilities of observing events with i clicks regardless the bin in which they occur. (b) Spatially multiplexed detector: the input beam is split by a set of beam splitters onto a collection of spatial modes. (c) Time-multiplexed detector: the input beam is coupled in a single-mode fibre and split on a first 50:50 beam splitter. The two arms are then recombined to form an unbalanced Mach-Zehnder interferometer with a relative delay $\Delta t = 50$ ns. This produces four distinct modes: two time bins on two distinct spatial modes. This operation is repeated in a second unbalanced interferometer with double relative delay $2\Delta t$, in order to produce two more time bins. This is the detector we adopted in the present experiments.

the input into two spatial and four temporal modes, whose separation is larger than the typical dead time of an avalanche photodiode [23,24,26,27].

The question arises whether there exists a way of observing nonclassicality directly in the measured quantities $\{c_i\}$. A solution can be found by inspecting the Mandel parameter:

$$Q_M = \frac{\Delta^2 n}{\bar{n}} - 1. \qquad (1)$$

The negativity of this parameter establishes a sufficient criterion for nonclassicality: this implies that the mean $\bar{n} = \sum_{n=0}^{\infty} n p_n$ is larger than the variance $\Delta^2 n = \sum_{n=0}^{\infty} (n - \bar{n})^2 p_n$, i.e., if the statistics are sub-Poissonian. Coherent states, which benchmark classical light, display Poissonian number statistics. By contrast, Fock states display sub-Poissonian statistics; hence, the corresponding Mandel parameter takes negative values. When using TMDs, a Poissonian distribution of the photons $\{p_n\}$ results in a binomial distribution of the counts $\{c_i\}$ [25,29]. Based on this, Sperling, Vogel, and Agarwal (SVA) have

developed a different nonclassicality criterion applying to the measured click statistics:

$$Q_B = \frac{\Delta^2 c}{\frac{\bar{c}}{N}\left(1 - \frac{\bar{c}}{N}\right)} - 1, \qquad (2)$$

where $\bar{c} = \sum_{i=0}^{N} i c_i$, and $\Delta^2 c = \sum_{i=0}^{N} (i - \bar{c})^2 c_i$. This extends Mandel's formula (1) to the case of a binomial distribution with mean x, the variance of which is given by $x(1 - x)$. Consequently, nonclassicality can be directly inferred from the sub-binomial behavior of the observed statistics, i.e., $Q_B < 0$.

Here, we experimentally measure both Q_B and Q_M for families of quantum states that may be tuned continually between the classical and nonclassical regimes. To obtain such states, we interfere a single photon with a coherent state on a beam splitter with variable reflectivity R, and consider the state on the transmitted arm conditioned on the presence of k photons on the reflected arm [33,34]. For $k = 1$, we produce non-Gaussian states by performing photon catalysis [27,35]. These allow us to investigate the behavior of Q_B in the experiment, as we tune the state from a single photon ($R = 1$) to a coherent state ($R = 0$).

The experimental scheme is shown in Fig. 2(b): a single photon is produced by pulsed parametric down-conversion in a nonlinear potassium dihydrogen phosphate (KDP) crystal. This interaction produces a pair of photons with orthogonal polarisations in a spectrally factorable state [36]: the horizontally (H) polarized photon is detected by an APD and serves as a herald event. The vertically polarized (V) photon is spatially overlapped with a coherent state $|\alpha\rangle$, H-polarized, on a polarizing beam splitter (PBS). A variable beam splitter, comprising a half-wave plate and a second PBS, is then used to interfere the two beams. We monitor one output port heralding on the measurement of either $k = 0$, or $k = 1$ photons by a first TMD. The conditional state on the second port constitutes our quantum signal, and the complete click statistics from a second TMD $\{c_i\}$ are collected.

We perform three different statistical analyses on the collected data, whose results are reported in Fig. 3(a) for $k = 0$, and in Fig. 3(b) for $k = 1$. In the first analysis, we assess the sub-Poissonian character of the click statistics using a Mandel-like parameter (red squares) defined as

$$Q_F = \frac{\Delta^2 c}{\bar{c}} - 1. \qquad (3)$$

The blue dots report the experimental result for the genuine Mandel parameter Eq. (1), after the photon distribution has been obtained by inversion [28]. Finally, the experimental values for the binomial parameter Eq. (2) are shown as the black squares.

In general, the Mandel-like parameter Q_F cannot be used to detect nonclassicality, as it can take negative values even for the coherent states obtained when $R \sim 0$ [25], as shown in Fig. 3(b). Further, its behavior depends on the particular class of states under investigation: for the case in
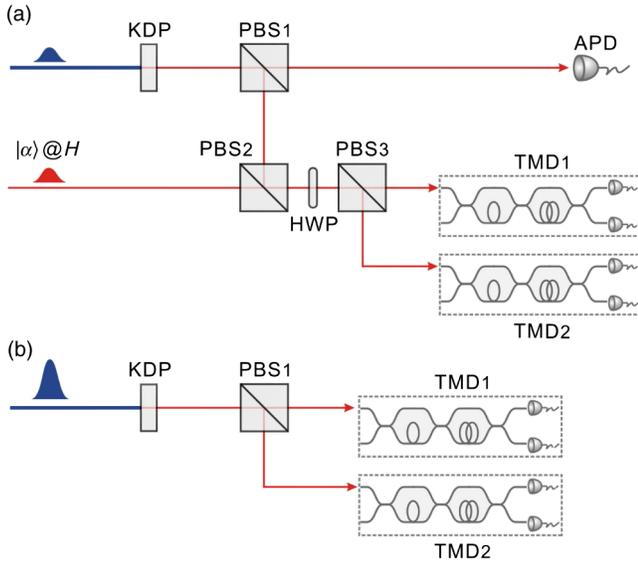
FIG. 2 (color online).   (a) Measurement of the nonclassicality of a single-mode state. Photons are produced by pulsed type-II colinear parametric down-conversion in a KDP crystal driven by a doubled Ti:Sa pump laser ($\lambda_p = 415$ nm, $\Delta\lambda = 50$ nm, repetition rate 256 kHz). This produces pairs of in a single spatio-temporal mode [36]. The presence of a photon in the V mode reflected by PBS_1 is heralded by a click of an APD on the H mode, and a trigger derived from the driving laser. A coherent state $|\alpha\rangle$, derived from the main laser, is made to interfere with the single photon on a variable beam splitter consisting of PBS_2, a half-wave-plate (HWP), and PBS_3. The effective reflectivity of the device is then set by the angle θ of the HWP as $R = \cos^2\theta$. The transmitted arm is delivered to detector TMD_1 which provides a second herald event, either no clicks $k = 0$ or a single click $k = 1$. The conditional states on the reflected arm are then analysed by TMD_2. (b) Observing sub-binomial behaviors in the joint click statistics from a two-mode squeezed state generated from the same crystal at higher pump intensity. The two modes from the KDP are directly delivered onto two detectors TMD_1 and TMD_2, and clicks are collected.

Fig. 3(a) the separation between this parameter and the Mandel parameter can be significant, while they are closer in Fig. 3(b). In both cases, a systematic failure of Q_F can be seen at low reflectivities. This issue is resolved by employing the binomial parameter Q_B, which performs as well as the Mandel parameter Q_M for our eight-bin detector, and with similar uncertainties. In our experiment, we have investigated an intensity regime in which the inversion is not affected by the high-order time bins, in order to have a reliable quantity of comparison for the SVA parameter of our states. However, this might not be feasible in the general case, as uncertainties in these terms will propagate badly in the reconstructed $\{p_n\}$. Thus the direct approach of SVA is useful in avoiding this source of error, as well instabilities arising from noise.

We also use the SVA parameter to characterize the output from the down-converter at higher gain, producing a two-mode squeezed state of the form
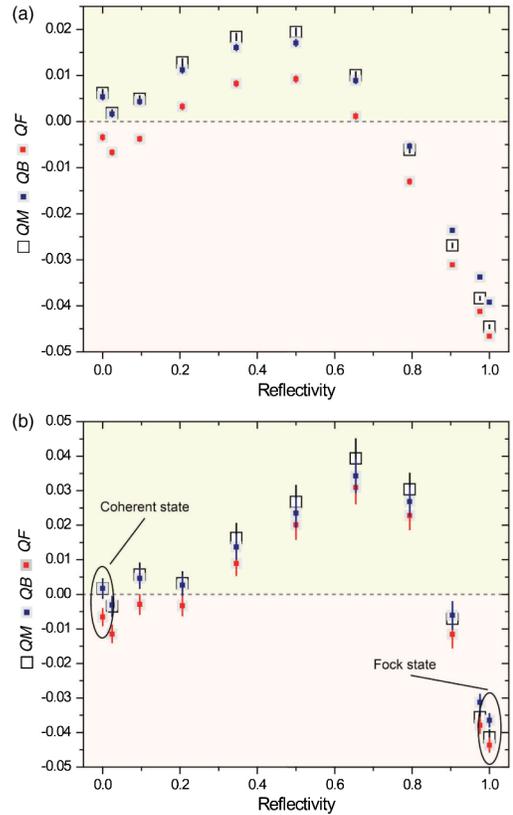
FIG. 3 (color online).   Test of nonclassicality for single-mode states heralded by (a) $k = 0$, and (b) $k = 1$. In both figures, the black boxes show the the Mandel parameter Q_M and the blue points show the SVA parameter Q_B. The values of the Mandel-like parameter calculated from the clicks Q_F are shown as red points. The limit $R \sim 0$ correspond to coherent states for which one expects no nonclassicality, while around $R \sim 1$, the states approximate displaced single photons [27]. All experimental points are obtained by 600 s of data collection. Errors are evaluated by a Monte Carlo technique assuming Poissonian noise.

$|\psi\rangle \propto \sum_{n\geq 0} \lambda^n |n\rangle_H |n\rangle_V$ on the two orthogonally polarized output modes. If we were to use a photon-number resolving detector, the observation of n photons on the H mode would imply the presence of n photons, hence a sub-Poissonian state, on the V mode [37,38]. In our experiment, as shown in Fig. 2(b), we observe a similar behavior in terms of sub-binomial light: a click from a TMD projects the other mode on to a sub-binomial state. The joint statistics from two TMDs, each measuring a different polarization mode is shown in Fig. 4(a): from this we have performed the SVA test on the states obtained by conditioning on a given number of clicks on one TMD or the other.

When all the events of TMD_2 are considered regardless of the measurement result at TMD_1, or vice versa, we observe classical behavior, as expected for a thermal state [Fig. 4(b)]: we obtain the values $Q_B = (9.3 \pm 0.6) \times 10^{-3}$ for the state on mode 1, and $Q_B = (10.9 \pm 0.6) \times 10^{-3}$ for
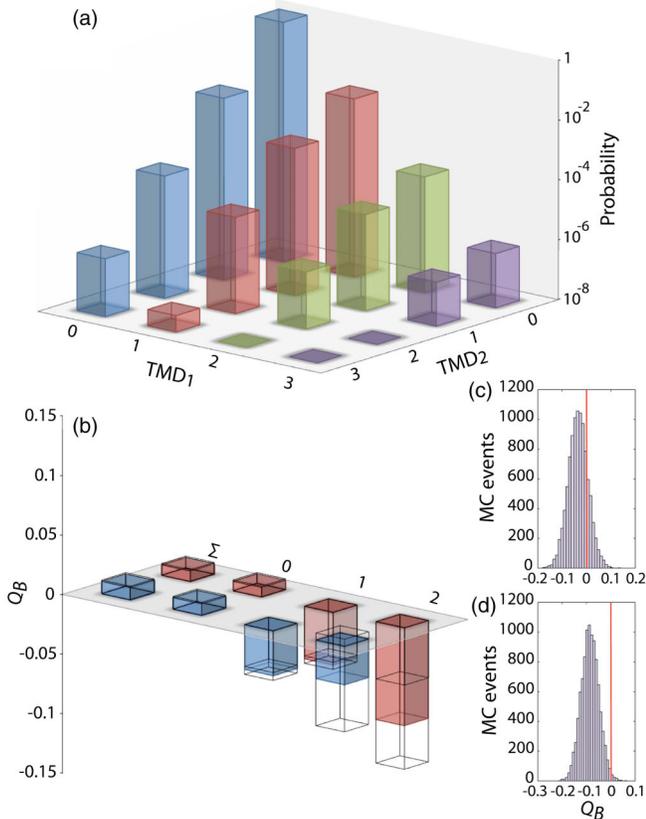
FIG. 4 (color online). (a) Joint statistics for detection with TMD on two-mode squeezed states, due to limited efficiency ($\sim 7\%$), the most frequent event is when no clicks are registered at either side. All the events in coincidence with a trigger signal from the main laser are included; (b) Measured Q_B parameter for the state detected by TMD_2 conditioned on different click events on TMD_1 (c) Statistical analysis of the Q_B parameter when conditioning on two clicks from TMD_2 (left), and TMD_1 (right). The histograms are obtained based on 10^4 Monte Carlo simulations assuming Poissonian noise.

the state on mode 2. Discrepancies with respect to the expected symmetry can be attributed to the different detection efficiencies which have been measured. When only the events causing no clicks on TMD_1 are registered, we still observe a similar behavior: the reduced efficiency of our detector, in fact, makes this event similar to tracing out the other mode. The measured values are $Q_B = (10.2 \pm 0.6) \times 10^{-3}$ (mode 1) and $Q_B = (8.5 \pm 0.6) \times 10^{-3}$ (mode 2). When single clicks are considered as heralds, the state becomes sub-binomial, and so it happens independently of the mode we use as the trigger: $Q_B = (-3.84 \pm 0.33) \times 10^{-2}$ (mode 1), and $Q_B = (-4.49 \pm 0.30) \times 10^{-2}$ (mode 2). Finally, when triggering on two clicks, the state does present some evidence for nonclassicality, $Q_B = (-3.3 \pm 3.9) \times 10^{-2}$ (mode 1) and $Q_B = (-8.3 \pm 3.5) \times 10^{-2}$ (mode 2), although the low counts allow us to be confident only for mode 2. A statistical analysis conducted by simulating experiments using a

Monte Carlo technique is reported in Fig. 4(c): while the most likely values for both modes do lie well below zero, the tails of the distribution make the value of Q_B for mode 1 still compatible with positive values.

Our experimental results, in the light of the retrodictive approach in Ref. [39], also provides preliminary evidence for a test of nonclassicality of the TMDs themselves. In the retrodictive framework, the nonclassicality of a detector D can be ascertained by observing the nonclassicality of one mode of $|\psi\rangle$ when the other mode is projected by the action of D in the limit of high squeezing $\lambda \to 1$. Although we are far from this regime, the observed negativity of Q_B resulting from conditioning one of the arms on a TMD points towards the nonclassicality of the device.

The direct experimental observation of the nonclassicality of light fields is a vital aspect of foundational studies and technological applications of quantum mechanics. In this work we have shown how this is made possible by the use of time-multiplexed detectors, and by directly inspecting the resulting click statistics. This represents a more elegant and unambiguous procedure for confirming quantumness than their indirect verification by deconvolving the action of the detector.

[1] E. P. Wigner, Phys. Rev. **40**, 749 (1932).
[2] R. J. Glauber, Phys. Rev. Lett. **10**, 84 (1963).
[3] E. C. G. Sudarshan, Phys. Rev. Lett. **10**, 277 (1963).
[4] W. Vogel and D.-G. Welsch, *Quantum Optics* (Wiley-VCH, Weinheim, 2006), 3rd ed.
[5] L. Mandel, Opt. Lett. **4**, 205 (1979).
[6] A. I. Lvovsky, H. Hansen, T. Aichele, O. Benson, J. Mlynek, and S. Schiller, Phys. Rev. Lett. **87**, 050402 (2001).
[7] A. Zavatta, S. Viciani, and M. Bellini, Science **306**, 660 (2004).
[8] A. Ourjoumtsev, R. Tualle-Brouri, J. Laurat, and P. Grangier, Science **312**, 83 (2006).
[9] A. Ourjoumtsev, H. Jeong, R. Tualle-Brouri, and P. Grangier, Nature (London) **448**, 784 (2007).
[10] A. Zavatta, V. Parigi, and M. Bellini, Phys. Rev. A **75**, 052106 (2007).
[11] K. Laiho, K. N. Cassemiro, D. Gross, and C. Silberhorn, Phys. Rev. Lett. **105**, 253603 (2010).
[12] A. Mari, K. Kieling, B. M. Nielsen, E. S. Polzik, and J. Eisert, Phys. Rev. Lett. **106**, 010403 (2011).
[13] R. Short and L. Mandel, Phys. Rev. Lett. **51**, 384 (1983).
[14] J. G. Rarity, P. R. Tapster, and E. Jakeman, Opt. Commun. **62**, 201 (1987).

[15] G. Zambra, A. Andreoni, M. Bondani, M. Gramegna, M. Genovese, G. Brida, A. Rossi, and M. Paris, Phys. Rev. Lett. **95,** 063602 (2005).

[16] A. B. U'Ren, C. Silberhorn, J. L. Ball, K. Banaszek, and I. A. Walmsley, Phys. Rev. A **72,** 021802(R) (2005).

[17] F. Bussires, J. A. Slater, N. Godbout, and W. Tittel, Opt. Express **16,** 17 060 (2008).

[18] M. Avenhaus, H. Coldenstrodt-Ronge, K. Laiho, W. Mauerer, I. A. Walmsley, and C. Silberhorn, Phys. Rev. Lett. **101,** 053601 (2008).

[19] E. Waks, E. Diamanti, B. C. Sanders, S. D. Bartlett, and Y. Yamamoto, Phys. Rev. Lett. **92,** 113602 (2004).

[20] T. Gerrits, S. Glancy, T. S. Clement, B. Calkins, A. E. Lita, A. J. Miller, A. L. Migdall, Sae Woo Nam, R. P. Mirin, and E. Knill, Phys. Rev. A **82,** 031802 (2010).

[21] T. Gerrits *et al.*, Phys. Rev. A **84,** 060301 (2011).

[22] G. Brida, L. Ciavarella, I. P. Degiovanni, M. Genovese, L. Lolli, M. G. Mingolla, F. Piacentini, M. Rajteri, E. Taralli, and M. G. A. Paris, New J. Phys. **14,** 085001 (2012).

[23] D. Achilles, C. Silberhorn, C. Śliwa, K. Banaszek, and I. A. Walmsley, Opt. Lett. **28,** 2387 (2003).

[24] J. S. Lundeen, A. Feito, H. Coldenstrodt-Ronge, K. L. Pregnell, Ch. Silberhorn, T. C. Ralph, J. Eisert, M. B. Plenio, and I. A. Walmsley, Nat. Phys. **5,** 27 (2008).

[25] J. Sperling, W. Vogel, and G. S. Agarwal, Phys. Rev. A **85,** 023820 (2012).

[26] M. Avenhaus, K. Laiho, M. V. Chekhova, and C. Silberhorn, Phys. Rev. Lett. **104,** 063602 (2010).

[27] T. J. Bartley, G. Donati, J. B. Spring, X.-M. Jin, M. Barbieri, A. Datta, B. J. Smith, and I. A. Walmsley, Phys. Rev. A **86,** 043820 (2012).

[28] A. Worsley, H. B. Coldenstrodt-Ronge, J. S. Lundeen, P. J. Mosley, B. J. Smith, G. Puentes, N. Thomas-Peter, and I. A. Walmsley, Opt. Express **17,** 4397 (2009).

[29] J. Sperling, W. Vogel, and G. S. Agarwal, Phys. Rev. Lett. **109,** 093601 (2012).

[30] P. Kok and S. L. Braunstein, Phys. Rev. A **63,** 033812 (2001).

[31] K. Banaszek and I. A. Walmsley, Opt. Lett. **28,** 52 (2003).

[32] L. Zhang, H. B. Coldenstrodt-Ronge, A. Datta, G. Puentes, J. S. Lundeen, X.-M. Jin, B. J. Smith, M. B. Plenio, and I. A. Walmsley, Nat. Photonics **6,** 364 (2012).

[33] K. Watanabe and Y. Yamamoto, Phys. Rev. A **38,** 3556 (1988).

[34] G. S. Agarwal, Quantum Opt. **2,** 1 (1990).

[35] A. I. Lvovsky and J. Mlynek, Phys. Rev. Lett. **88,** 250401 (2002).

[36] P. J. Mosley, J. Lundeen, B. Smith, P. Wasylczyk, A. U'Ren, C. Silberhorn, and I. A. Walmsley, Phys. Rev. Lett. **100,** 133601 (2008).

[37] H. B. Coldenstrodt-Ronge *et al.*, *Joint Photon Statistics of Photon-Subtracted Squeezed Light* (IEEE, Baltimore, MD, 2009).

[38] L. Dovrat, M. Bakstein, D. Istrati, E. Megidish, A. Halevy, and H. S. Eisenberg, arXiv:1210.0751.

[39] T. Amri, J. Laurat, and C. Fabre, Phys. Rev. Lett. **106,** 020502 (2011).